Clarification of the Mechanism of Acylation Reaction and Origin of Substrate Specificity of the Serine-Carboxyl Peptidase Sedolisin through QM/MM Free Energy Simulations

Qin Xu,[†] Jianzhuang Yao,[†] Alexander Wlodawer,[‡] and Hong Guo*,[†]

[†]Department of Biochemistry and Cellular and Molecular Biology, University of Tennessee, Knoxville, Tennessee 3799, United States

[‡]Protein Structure Section, Macromolecular Crystallography Laboratory, National Cancer Institute at Frederick, Frederick, Maryland 21702, United States

ABSTRACT: Quantum mechanical/molecular mechanical (QM/MM) free energy simulations are applied for understanding the mechanism of the acylation reaction catalyzed by sedolisin, a representative serine-carboxyl peptidase, leading to the acyl-enzyme (AE) and first product from the enzyme-catalyzed reaction. One of the interesting questions to be addressed in this work is the origin of the substrate specificity of sedolisin that shows a relatively high activity on the

substrates with Glu at P_1 site. It is shown that the bond making and breaking events of the acylation reaction involving a peptide substrate (LLE*FL) seem to be accompanied by local conformational changes, proton transfers as well as the formation of alternative hydrogen bonds. The results of the simulations indicate that the conformational change of Glu at P_1 site and its formation of a low barrier hydrogen bond with Asp-170 (along with the transient proton transfer) during the acylation reaction might play a role in the relatively high specificity for the substrate with Glu at P_1 site. The role of some key residues in the catalysis is confirmed through free energy simulations. Glu-80 is found to act as a general base to accept a proton from Ser-287 during the nucleophilic attack and then as a general acid to protonate the leaving group (N—H of $P_{1'}$-Phe) during the cleavage of the scissile peptide bond. Another acidic residue, Asp-170, acts as a general acid catalyst to protonate the carbonyl of P_1-Glu during the formation of the tetrahedral intermediate and as a general base for the formation of the acyl-enzyme. The energetic results from the free energy simulations support the importance of proton transfer from Asp-170 to the carbonyl of P_1-Glu in the stabilization of the tetrahedral intermediate and the formation of a low-barrier hydrogen bond between the carboxyl group of P_1-Glu and Asp-170 in the lowering of the free energy barrier for the cleavage of the peptide bond. Detailed analyses of the proton transfers during acylation are also given.
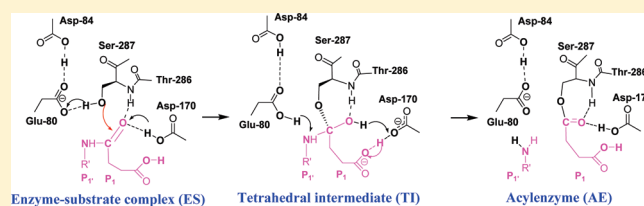
■ INTRODUCTION

Sedolisins (serine-carboxyl peptidases) belong to the family S53 of clan SB of serine peptidases (MEROPS S53).[1] The enzymes in this family share some common properties, including maximum activity at low pH (e.g., pH 3—5) and the presence of conserved acidic residues (aspartate and glutamate) required for the activity.[1c,2] The members of the family also include tripeptidyl-peptidase 1 (TPP1)[3] for which the loss of the activity as a result of mutations in the TPP1 gene (previously named CLN2) is believed to be the cause of a fatal neurodegenerative disease, classical late-infantile neuronal ceroid lipofuscinosis.[3,4]

As the first isolated and described member of the sedolisins family, *Pseudomonas* sp. 101 sedolisin has been extensively studied by biochemical and mutagenesis approaches along with the determination of crystal structures for several enzyme—inhibitor complexes;[1b,5] a quantum mechanical/molecular mechanical (QM/MM) study based on energy minimization approach has also been performed on this enzyme.[6] Sedolisin has a catalytic triad Ser-287-Glu-80-Asp-84 in place of the Ser-His-Asp triad of related (but usually smaller) classical serine peptidases.

Another conserved acidic residue, Asp-170, is structurally equivalent to Asn-155 (part of the oxyanion hole) in subtilisin. The natural substrates for most of the serine carboxyl peptidases are still unknown. Some understanding of the substrate specificity for these enzymes has been achieved through inspection of the inhibitor interactions in the X-ray structures of these enzymes, and/or from the determination of their ability to process peptide libraries.[1b,1c,5d,5e,7] Nevertheless, the origin of differences in substrate preferences for different members of the sedolisin family is still not well understood. For instance, the analysis of the cleavage of peptides in two separate libraries (13 718 peptides) for sedolisin showed that the substrates with Glu at P_1 site tend to have a higher specificity than substrates with some other residues (e.g., Gln and Arg). For kumamolisin-As, another member of the family, a relatively high specificity for the substrates with a positively charged residue at P_1 (e.g., His or

Arg) was observed by specificity profile analysis using a peptide library.[7a] The experimental data on the substrate specificity are often difficult to explain, and computational investigations might provide some useful insights.

We have previously performed QM/MM free energy (potential of mean force) simulations on kumamolisin-As (in which the catalytic triad consists of Ser-287-Glu-78-Asp-82, and Asp-164 corresponds to Asp-170 in sedolisin).[8] It was found that the active site dynamics and proton transfers can be of importance for the efficiency of the catalysis as well as the substrate specificity. One result from the computer simulations that is of considerable interest is that Asp-164 in kumamolisin-As seemed to act as a general acid catalyst to protonate the substrate and stabilize the tetrahedral intermediate (TI) during the nucleophilic attack by the serine residue. Asp-164 was also found to act as a general base during the formation of the acyl-enzyme.[8a,8d] A similar result was obtained for sedolisin from QM/MM investigations using energy minimization approach,[6] even though some mechanistic differences appear to exist between the two computational studies. Thus, although sedolisins might have evolved from a common precursor of classical serine peptidases, they seem to have ended up with the use of some of the chemistry of aspartic peptidases for the catalysis. Another interesting suggestion from the previous computer simulations on the acylation step of the kumamolisin-As catalysis is that the dynamics involving the His side chain of the substrate at P_1 triggered by the bond-breaking and -making events might play an important role in the stabilization of the tetrahedral intermediate (TI1) through dynamic substrate-assisted catalysis (DSAC). It was suggested[8c,8d] that the DSAC effect could contribute to the relatively high specificity for the substrates with His at P_1 as observed experimentally for kumamolisin-As. Interestingly, the effect of DSAC seems to be less important for deacylation than for acylation,[8e] and a detailed investigation is still necessary.

In this paper, we investigate the acylation reaction of a five-residue peptide (LLE*FL) catalyzed by sedolisin using QM/MM free energy (potential of mean force) simulations. Consistent with previous suggestions[1b,1c,5d,5e] and earlier computational results,[6,8] Glu-80 is found to act as a general acid/base catalyst to shuffle the proton from Ser-287 to the leaving group of the acylation reaction. The energetic results from the free energy simulations support importance of the proton transfer from Asp-170 to the carbonyl of P_1-Glu in the stabilization of the tetrahedral intermediate and the formation of a low-barrier hydrogen bond between the P_1-Glu side chain and Asp-170 in the lowering of the free energy barrier at the transition state for the cleavage of the scissile peptide bond through dynamic substrate-assisted catalysis (DSAC). Detailed analyses of the proton transfers during acylation are also given.

■ METHOD

The available X-ray structures for sedolisins do not contain actual substrates at the active site, whereas such structures (models) of the enzyme—substrate complexes are required for computational investigations of catalytic mechanisms of the acylation reactions. In our previous studies of kumamolisin-As,[8c—8e] the X-ray structure for the S278A mutant of pro-kumamolisin (PDB ID 1T1E, resolution 1.18 Å)[7c] was used to help to generate the enzyme—substrate complex for performing the computer simulations. Specifically, the structures of the kumamolisin-As-inhibitor (AcIPF) complex and the catalytic domain of the S278A mutant of

pro-kumamolisin were first superposed, and the coordinates of the P_3-Arg-169p-P_2-Pro-170p-P_1-His-171p-P_1'-Phe-172p-P_2'-Arg-173p peptide fragment from the linker of the S278A mutant of pro-kumamolisin were initially used to generate the coordinates of the GPH*FF substrate. For sedolisin, the experimental structure of pro-sedolisin is not available. Fortunately, previous structural studies have shown that the structures for kumamolisin and sedolisin are extremely similar, especially in the cores.[1c,5e,7a] Therefore, the X-ray structure of sedolisin complexed with the inhibitor pseudoiodotyrostatin (PDB ID: 1NLU, resolution 1.3 Å)[5e] and the X-ray structure of the S287A mutant of pro-kumamolisin (PDB ID: 1T1E, resolution 1.8 Å)[7c] were superposed to produce the initial structure for the substrate (see ref 8 for more details). This step was followed by manual mutations of the linker peptide (RPHFR) in pro-kumamolisin to generate LLE*FL using the MOE package.[9] Here LLE*FL was selected as the substrate for this investigation because sedolisin seems to have a relatively high catalytic efficiency for such a substrate based on the specificity assay study.[5e] The other part of 1T1E and the two inhibitors of 1NLU were then removed, and the resulting structure of the enzyme—substrate complex was subject to energy minimization and structural refinement. The coordinates of sedolisin and the LLE*FL peptide were then combined together to generate the putative sedolisin—substrate complex used to initiate the computational studies. The structures for the enzyme—substrate complexes of the D170N and D170A mutants were generated by making the corresponding mutations manually in the enzyme—substrate complex of the wild-type enzyme (see above). The structure of the wild-type enzyme complex containing the LLQ*FL substrate was generated by replacing P_1-Glu by Gln. To determine whether the structure of the enzyme—substrate complex generated above is consistent with the experimental structural data,[5e] the acyl-enzyme complex obtained from the free energy simulations (see below) was superposed with the X-ray structure of the sedolisin-inhibitor complex (PDB ID: 1NLU). This sedolisin-inhibitor complex has two molecules of pseudoiodotyrostatin bound at the active site with the first one covalently connecting to Ser-287 of sedolisin through its aldehyde functional group. Therefore, the backbone conformation of the first pseudoiodotyrostatin molecule might be considered as a mimic of the P_3-P_2-P_1 residues from the substrate after the acylation reaction. (Note that the side chains of the P_3, P_2, and P_1 residues used in this study are not the same as those in pseudoiodotyrostatin, and a complete structural comparison is therefore not possible.) It was found that the backbone atoms of the P_3-P_2-P_1 residues (LLE) from the acyl-enzyme could be superposed with those of the first pseudoiodotyrostatin molecule in the X-ray structure extremely well with rms deviations of only 0.1—0.2 Å. This result indicates that the structure of the enzyme—substrate complex used for the simulations is meaningful.

The constructed structures of the enzyme—substrate complexes were solvated by a modified TIP3P water model[10] using the CHARMM35b1 program.[11] The stochastic boundary MD method[12] was applied to the solvated system. The system was partitioned into the reaction zone and the reservoir region; the reaction zone was further divided into the reaction region and the buffer region. The reaction region contains the system with radius $R < 16$ Å, and buffer region had R equal to 16 Å $\leq R \leq$ 18 Å. The reference center for this partitioning was chosen to be the carbonyl carbon atom of the residue at P_1 site of the substrate. The buffer region was simulated with Langevin dynamics (LD), and the reaction region with molecular dynamics (MD). The side

chains of Glu-80, Asp-84, Asp-170, and Ser-287, along with a part of the substrate (i.e., the carbonyl of P_2 residue, the whole P_1 residue, and C_α and amide group of $P_{1'}$ residue) were treated by QM method; the rest of the system was treated by MM method. The QM method used in this study was the Self-Consistent Charge Density Functional Tight Binding (SCC-DFTB)[13] method implemented in the CHARMM program, and this method has been applied previously in the studies of a number of models and enzyme systems,[14] including kumamolisin-As.[8a−8c] High-level ab initio methods (e.g., B3LYP and MP2) are too time-consuming to be used for MD and free energy simulations, although test calculations based on the energy-minimization approach with a high level QM (B3LYP)/MM method was used previously in our study of kuma-molisin-As.[8a] The all-hydrogen potential function (PARAM22)[15] was used for the MM method. The link-atom approach[16] available in the CHARMM program was employed to separate the QM and MM regions. The resulting system contains around 3500 atoms.

The initial structure for the stochastic boundary system was optimized by adopted basis Newton−Rhaphson (ABNR) method.[12] The system was gradually heated from 50 to 300 K in 20 ps and equilibrated at 300 K for 70 ps. MD simulations were then performed at 300 K for more than 1 ns. The time step for integration of the equations of motions was selected to be 1 fs. The coordinates were saved every 50 fs for the analysis of the dynamical properties of the systems. The Langevin dynamics in the buffer region had frictional constants as 250 ps^{-1} for the protein atoms and 62 ps^{-1} for the water molecules.

To determine the free energy changes (potential of mean force, or PMF) from the enzyme−substrate complex to the acyl-enzyme, the umbrella sampling method[17] implemented in the CHARMM program[18] was applied. The reaction coordinate was defined as the difference between the distances of the scissile peptide bond, $R(C-N)$, and the nucleophilic attack, $R[C \cdots O_\gamma(Ser-287)]$. This reaction coordinate allows the description of the nucleophilic attack and cleavage of the scissile peptide bond with ξ increasing from −0.95 to 0.95 Å in about 20 windows. The determination of multidimensional free energy maps would be too time-consuming. Our previous study[8b] indicated that the one-dimensional free energy simulations with the selection of a suitable reaction coordinate reflecting the key chemical events may be able to capture the key energetic properties for the reaction (e.g., the free energy barrier). The weighted histogram analysis method (WHAM) was applied to determine the change of the free energy (PMF) for the acylation reaction. For each window, 100 ps simulations were performed (50 ps equilibrium and 50 ps production run). The simulations of five selected windows corresponding to the five different stages of acylation (ES, TS1, TI, TS2, and AE) were extended to 1 ns to explore possible structural changes. To understand the importance of the proton transfers between Asp-170 and P_1-Glu, two more free energy profiles were obtained for the wild-type enzyme complexed with LLE*FL for which the proton on the carboxyl group of Asp-170 or P_1-Glu was fixed, respectively, using the SHAKE algorithm.[19] In addition, the free energy profiles were also obtained for the D170N and D170A mutants complexed with LLE*FL as well as the wild-type enzyme with the LLQ*FL substrate (i.e., Glu at P_1 is replaced by Gln). The force constants for umbrella samplings were in the range of 100−800 kcal·Mol^{-1}·Å^{-2}.

■ RESULTS AND DISCUSSION

The average active-site structure of the substrate (LLE*FL) complex for wild-type sedolisin obtained from the MD simulations is plotted in Figure 1A (left). The fluctuations of certain distances involving protons H_a, H_b, H_c, and H_d during the simulations (i.e., the distances of a given proton to nearby oxygen atoms or nitrogen atom as a function of time) are also given (Figure 1A, right). Ser-287 is expected to attack the carbonyl carbon atom of the substrate. Consistent with this role, Ser-287 is well aligned with the substrate with a distance of 2.3 Å from the carbonyl carbon atom of P_1-Glu for the nucleophilic attack. Figure 1A also shows that Glu-80 forms a strong hydrogen bond with the hydrogen atom (H_a) of Ser-287 and is therefore expected to act the general base during the nucleophilic attack. This sugges-tion is consistent with the results from previous studies.[1b,1c,5d,5e,6] Moreover, this residue forms a low-barrier hydrogen bond (LBHB) with Asp-84 involving H_b (Figure 1A, right, the second panel from the top). Indeed, H_b spends considerable time in the middle of the two carboxyl oxygen atoms from Glu-80 and Asp-84, respectively, with average distances of 1.4 and 1.1 Å to $O_{\varepsilon2}$(Glu-80) and $O_{\delta2}$(Asp-84). This LBHB along with the interactions involving Ser-133, Asn-131, and the backbone carbonyl group of Ser-287 may play an important role in maintaining the structural integrity of the active site. Asp-170 interacts with the carbonyl oxygen of P_1-Glu with its position stabilized by the hydrogen bonds from Thr-286 (both the side chain and backbone amide group). It has been suggested that the corresponding aspartate residue in kumamolisin-As may play a role as general acid/base catalysts during the acylation as well as deacylation steps;[8] a similar suggestion has also been made for Asp-170 in sedolisin,[6] although there are some mecha-nistic differences (see below).

The changes of free energy (potential of mean force) as a function of the reaction coordinate (ξ) for the acylation reaction involving the LLE*FL substrate in sedolisin (red solid line), D170N (green dashed line), and D170A (magenta dot-dashed line) are given in Figure 1B. The free energy profiles are also given for the cases in which Asp-170 is deprotonated (orange double-dot-dashed line) or the proton on protonated Asp-170 (H_c) is fixed by the SHAKE algorithm (blue dotted line). The purpose for the use of the SHAKE algorithm is to prevent Asp-170 from acting as the general acid catalyst for the nucleophilic attack, although it can still provide electrostatic stabilization of the tetrahedral intermediate (i.e., similar to the role of Asn-155 in subtilisin). Figure 1B shows that as the reaction coordinate [$\xi = R(C-N) - R(C-O_\gamma)$] increases from −0.95 to 0.95 Å, the wild-type enzyme complex with protonated Asp-170 and without the use of the SHAKE algorithm (i.e., red solid line) seems to follow two separate steps during acylation; that is, the nucleo-philic attack of Ser-287 on the substrate in the formation of a stable tetrahedral intermediate (TI) and the cleavage of the scissile peptide bond in the formation of the acyl-enzyme (see below for more discussion). Such bond breaking and making events are likely to change the charge distributions, leading to possible proton transfers, conformational changes, as well as formation of alternative hydrogen-bonding interactions at the active site. It is of interest to note from Figure 1B that preventing the proton transfer away from Asp-170 or mutating this residue to Asn leads to an increase of the free energy barrier of the acylation reaction by more than 10 kcal/mol. As a result, the stable tetrahedral intermediate along the reaction pathway dis-appeared. Thus, the electrostatic oxyanion hole interaction involving the protonated Asp-170 seems to be insufficient for generating a stable tetrahedral intermediate during catalysis. Similar results were also obtained from kumamolisin-As.[8d]
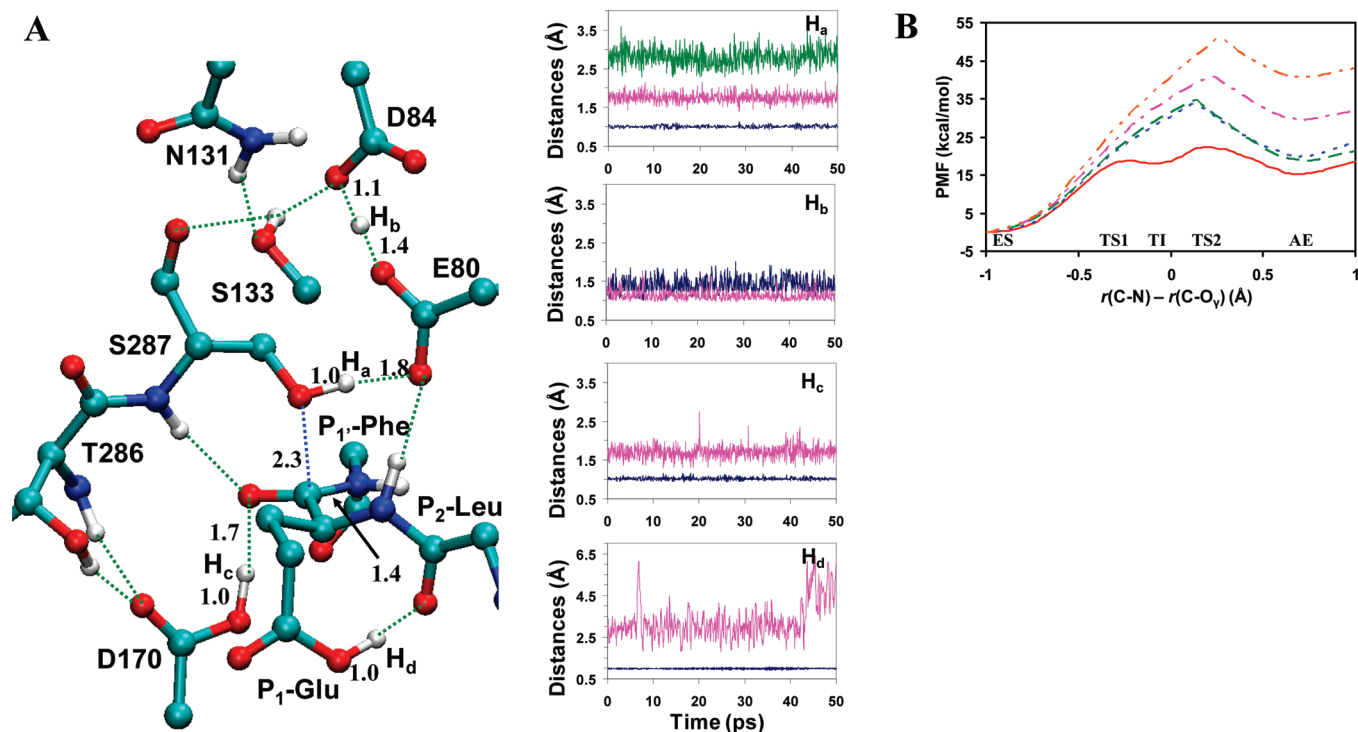
Figure 1. (A) The average active-site structure (left) and certain distance fluctuations (right) of the substrate (LLE*FL) complex for wild-type sedolisin obtained from the MD simulations. The distance involved in the nucleophilic attack is indicated with the blue dotted line and hydrogen bonds are shown in green dotted lines in the average structure. For clarity, the nonpolar hydrogen atoms are not shown. The four protons that may undergo transfer reactions during the acylation step are labeled as H_a, H_b, H_c, and H_d, and the related distance fluctuations during the MD simulations are monitored in the panels on the right. Top panel: $H_a \cdots O_\gamma$(Ser-287) (blue), $H_a \cdots O_{\varepsilon 1}$(Glu-80) (magenta), and $H_a \cdots N$($P_{1'}$-Phe) (green). The second panel from top: $H_b \cdots O_{\varepsilon 2}$(Glu-80) (blue) and $H_b \cdots O_{\delta 2}$(Asp-84) (magenta). The third panel from top: $H_c \cdots O_{\delta 1}$(Asp-170) (blue) and $H_c \cdots O$(P_1-Glu) (magenta). Bottom panel: $H_d \cdots O_{\varepsilon 2}$($P_1$-Glu) (blue) and $H_d \cdots O_{\delta 1}$(Asp-170) (magenta). (B) The free energy (potential of mean force) profiles of the acylation reaction involving LLE*FL peptide catalyzed by wild-type enzyme (red solid line), D170N mutant (green dash), and D170A mutant (magenta dot-dash). In addition, the free energy profiles for wild-type enzyme with H_c fixed on Asp-170 using SHAKE algorithm (blue dotted line) or with deprotonated Asp-170 (orange double-dot-dashed line) are also given. The reaction coordinate for the acylations is $\xi = R(C-N) - R(C \cdots O_\gamma)$; that is, the distance difference for the scissile peptide bond $R(C-N)$ and the nucleophilic attack $R[C \cdots O_\gamma(\text{Ser-287})]$. Certain structural and dynamic features at the five stages of the acylation reaction [reactant complex (ES), transition state for the nucleophilic attack (TS1), tetrahedral intermediate (TI), transition state for the peptide bond cleavage (TS2), and acyl-enzyme (AE)] are given in Figure 1A and 2(A–D), respectively.

Figure 1B also shows that the replacement of Asp-170 by Ala or use of deprotonated Asp-170 increases the free energy barrier considerably. The results of the simulations reported here support the earlier proposal[6,8a–8d] for the existence of the general acid mechanism in the stabilization of the tetrahedral intermediate. The results are also consistent with the available experimental data on the importance of Asp-170 for the activation, presumably through a similar general acid mechanism involving this residue. Indeed, the Asp-170→Ala mutation resulted in a complete loss of the enzyme activity, presumably due to the failure of the zymogen being converted to mature protein.[5c]

The average active-site structures at the different stages of the acylation reaction (i.e., TS1, TI, TS2, and AE) for wild-type are plotted in Figure 2 (i.e., corresponding to the red solid line in Figure 1B). Figure 2A,B shows that Glu-80 accepts H_a from the hydroxyl of Ser-287 during the nucleophilic attack, while Asp-170 donates its proton (H_c) to the carbonyl oxygen of P_1-Glu. Thus, these two residues play the roles of the general base and acid, respectively, during the formation of TI, consistent with the previous results on kumamolisin-As[8a,8b] and the suggestion from the earlier QM/MM study[6] on sedolisin based on energy minimization approach. There are, however, some mechanistic differences between the earlier study[6] of sedolisin and the present

work, based on the free energy simulations. For instance, one of the main differences is that in the earlier study the proton transfer from Asp-170 to the carbonyl oxygen of the P_1 residue is well ahead of the proton transfer from Ser-287 to Glu-80 (i.e., in a stepwise fashion).[6] Indeed, at TS1 the proton transfer from Asp-170 to the carbonyl oxygen of the P_1 residue was almost completed, while the proton transfer from Ser-287 to Glu-80 did not start yet (see Figure 7 of ref 6). By contrast, the results of the free energy simulations reported here showed that the two proton transfers seem to occur somewhat more concertedly (see Figure 2A for the structure and distance fluctuations at TS1). In fact, Figure 2A shows that the proton transfer from Ser-287 to Glu-80 appears slightly ahead of the proton transfer from Asp-170 to the P_1 residue, consistent with the earlier study on kumamolisin-As.[8] Some mechanistic differences also exist for the formation of the acyl-enzyme from TI. These differences in the results are probably due, at least in part, to the use of different computational approaches, although the use of different substrates for the studies (i.e., LLE*FL in the present study and RGFFYT in the earlier work) might also be a factor (see below).

Figure 2A shows that the distance of H_a to N of the $P_{1'}$-Phe backbone (the green line in the first panel from top in Figure 2A) was rather long (∼2.5 Å), suggesting that Glu-80 has not
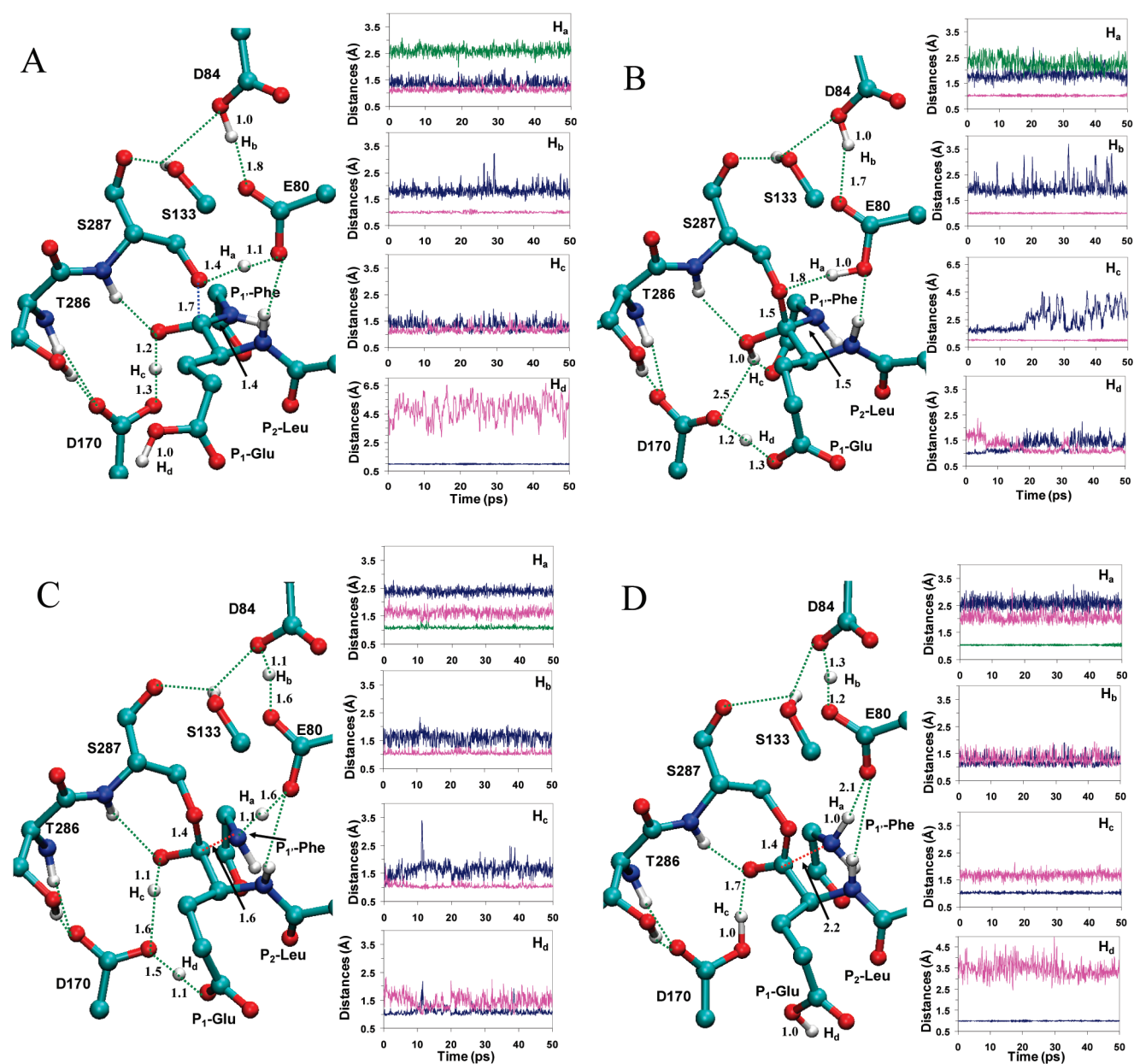
Figure 2. (A) The average structure of the transition state of the nucleophilic attack (left) and the distance fluctuations (right). See Figure 1A for explanations of the structures and color schemes for the distances involving H_a, H_b, H_c, and H_d. (B) The tetrahedral intermediate. (C) The transition state for the peptide bond cleavage. The distance of the peptide bond cleavage is indicated with red dotted lines. (D) Acyl-enzyme.

positioned itself for donating the proton to the leaving group at TS1. Interestingly, Figure 2B shows that the side chain of P_1-Glu undergoes a conformational change and forms a low barrier hydrogen bond involving H_d with Asp-170 at TI (see also the distance fluctuations in the first panel from the bottom on the right). Figure 2C,D shows that the protonation of the leaving group by Glu-80 involving H_a occurs during the cleavage of the scissile peptide bond, and the formation of the acyl-enzyme is accompanied by some other proton transfer or partial proton transfer processes. Specifically, a low-barrier hydrogen bond is formed between Asp-84 and Glu-80 (see the second panels from top in Figure 2C and D). Proton transfer/shift involving H_c and H_d were also observed during the formation of the acyl-enzyme in which Asp-170 acted as a general base to receive the proton (H_c) from the carbonyl oxygen of P_1-Glu and the side chain of

P_1-Glu picked up H_d. Such movements of the protons are expected to play a role in the catalysis (see below). The schematic figure for the catalytic mechanism obtained from the simulations is plotted in Figure 3A.

To determine as to whether the formation of the LBHB involving P_1-Glu could be a factor in the lowering of the energy barrier for the acylation reaction and relatively high-substrate specificity, free energy simulations were performed on additional models. The models include the sedolisin complex with the LLQ*FL substrate (instead of LLE*FL), as well as the original complex containing P_1-Glu with H_d fixed by the SHAKE algorithm. Moreover, a model with deprotonated P_1-Glu in the reactant complex (instead of protonated P_1-Glu) was also used. The reason for the use of deprotonated P_1-Glu in the latter case is because the side chain of P_1-Glu seemed to be in the position to
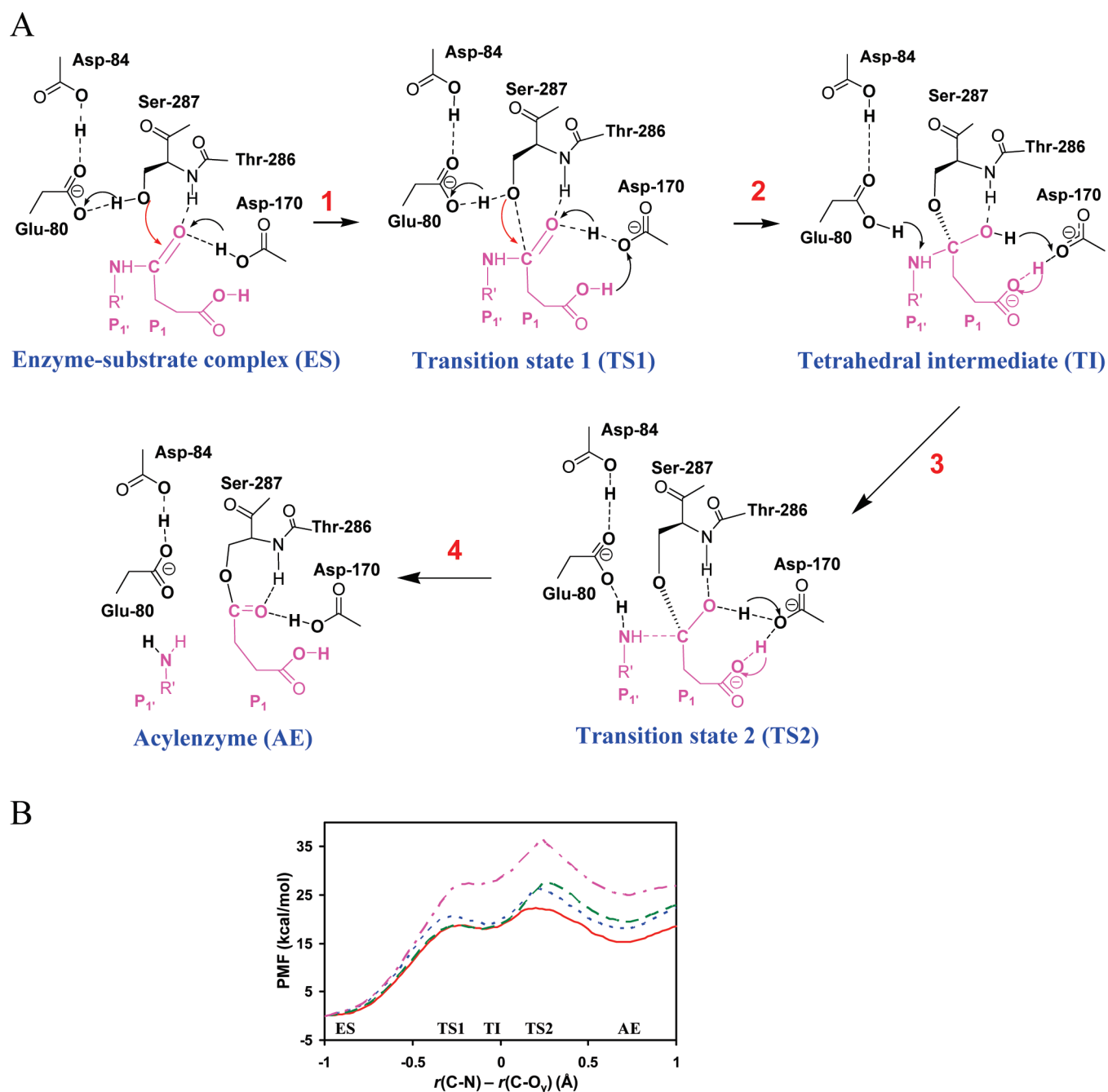
Figure 3. (A) The proposed mechanism for the acylation catalyzed by sedolisin based on the present study. (B) The free energy profiles of the acylation reaction for different substrates catalyzed by wild-type sedolisin. Red solid line: substrate LLE*FL with P_1-Glu protonated in the reactant complex (i.e., the red solid line from Figure 1B). Blue dotted line: P_1-Glu changed to Gln. Green dashed line: P_1-Glu with H_d fixed by the SHAKE algorithm. Magenta dot-dashed line: P_1-Glu in the deprotonated state with the original LLE*FL substrate. See Figure 1B for additional explanations.

form an ion pair with Arg-179. The formation of the ion pair might contribute to the relatively high specificity for the substrates with Glu at P_1 site,[5e] although other factors, such as the proton relay mentioned above, can be involved as well. It should be pointed out that Arg-179 also forms an ion pair with a nearby Glu-175 in the X-ray structure and in structures from the simulations. Thus, the effect of the interaction between the deprotonated P_1-Glu and Arg-179 on the chemical steps of the acylation reaction is unclear. The energetic information obtained from the simulations for the system with deprotonated P_1-Glu would be of interest. Figure 3B compares the free energy profiles

for the three additional models mentioned above with the one with LLE*FL and protonated P_1-Glu without the use of the SHAKE algorithm (i.e., the red solid line in Figure 1B). As is evident from Figure 3B, the free energy barrier for the cleavage of the scissile peptide bond increases by about 5 kcal/mol when P_1-Glu is replaced by P_1-Gln or H_d on P_1-Glu is fixed by the SHAKE algorithm. This seems to indicate that the local conformational change and formation of the low-barrier hydrogen bond through dynamic substrate-assisted catalysis (DSAC) might play a role in the relatively high specificity for the substrates with Glu at P_1. Figure 3B also shows that the free energy barrier for the case with

the deprotonated P$_1$-Glu is quite high, and this seems to suggest that the formation of the ion pair with Arg-179 is unlikely to be the reason for the relatively high specificity. Examination of the trajectories obtained from the free energy simulations showed that the deprotonated P$_1$-Glu formed a stable ion pair with Arg-179 and did not form strong interaction(s) with the groups (e.g., Asp-170) involved in the chemical process of the enzyme-catalyzed reaction.

CONCLUSIONS

QM/MM free energy simulations were applied to investigate the mechanism of the acylation reaction catalyzed by sedolisin and to understand the origin of the substrate specificity of sedolisin. It has been shown that the bond making and breaking events of the acylation reaction involving a peptide substrate (LLE*FL) seem to be accompanied by local conformational changes, proton transfers as well as the formation of alternative hydrogen bonds. The results of the simulations suggested that the proton relay involving Glu at P$_1$ site might lower the energy barrier for the cleavage of the scissile peptide bond and play a role in the relatively high specificity for the substrate with Glu at P$_1$ site. The role of some key residues in the catalysis has been confirmed by the free energy simulations. Glu-80 was found to act as a general base to accept a proton from Ser-287 during the nucleophilic attack and then as a general acid to protonate the leaving group (N—H of P$_{1'}$-Phe) during the cleavage of the scissile peptide bond. Another acidic residue, Asp-170, acted as a general acid catalyst to protonate the carbonyl of P$_1$-Glu during the formation of the tetrahedral intermediate and as a general base in the formation of the acyl-enzyme.

AUTHOR INFORMATION

Corresponding Author
*E-mail: hguo1@utk.edu.

ACKNOWLEDGMENT

REFERENCES

(1) (a) Oda, K.; Sugitani, M.; Fukuhara, K.; Murao, S. *Biochim. Biophys. Acta* **1987**, *923*, 463. (b) Wlodawer, A.; Li, M.; Dauter, Z.; Gustchina, A.; Uchida, K.; Oyama, H.; Dunn, B. M.; Oda, K. *Nat. Struct. Biol.* **2001**, *8*, 442. (c) Wlodawer, A.; Li, M.; Gustchina, A.; Oyama, H.; Dunn, B. M.; Oda, K. *Acta Biochim. Pol.* **2003**, *50*, 81.

(2) (a) Reichard, U.; Lechenne, B.; Asif, A. R.; Streit, F.; Grouzmann, E.; Jousson, O.; Monod, M. *Appl. Environ. Microbiol.* **2006**, *72*, 1739. (b) Siezen, R. J.; Renckens, B.; Boekhorst, J. *Proteins: Struct., Funct., Bioinf.* **2007**, *67*, 681. (c) Murao, S.; Ohkuni, K.; Nagao, M.; Hirayama, K.; Fukuhara, K.; Oda, K.; Oyama, H.; Shin, T. *J. Biol. Chem.* **1993**, *268*, 349. (d) Shibata, M.; Dunn, B. M.; Oda, K. *J. Biochem.* **1998**, *124*, 642. (e) Tsuruoka, N.; Nakayama, T.; Ashida, M.; Hemmi, H.; Nakao, M.; Minakata, H.; Oyama, H.; Oda, K.; Nishino, T. *Appl. Environ. Microbiol.* **2003**, *69*, 162. (f) Tsuruoka, N.; Isono, Y.; Shida, O.; Hemmi, H.; Nakayama, T.; Nishino, T. *Int. J. Syst. Evol. Microbiol.* **2003**, *53*, 1081.

(3) Sleat, D. E.; Donnelly, R. J.; Lackland, H.; Liu, C. G.; Sohar, I.; Pullarkat, R. K.; Lobel, P. *Science* **1997**, *277*, 1802.

(4) (a) Lin, L.; Sohar, I.; Lackland, H.; Lobel, P. *J. Biol. Chem.* **2001**, *276*, 2249. (b) Rawlings, N. D.; Barrett, A. J. *Biochim. Biophys. Acta* **1999**, *1429*, 496. (c) Golabek, A. A.; Kida, E. *Biol. Chem.* **2006**, *387*, 1091.

(5) (a) Ito, M.; Narutaki, S.; Uchida, K.; Oda, K. *J. Biochem.* **1999**, *125*, 210. (b) Oda, K.; Takahashi, T.; Tokuda, Y.; Shibano, Y.; Takahashi, S. *J. Biol. Chem.* **1994**, *269*, 26518. (c) Oyama, H.; Abe, S.; Ushiyama, S.; Takahashi, S.; Oda, K. *J. Biol. Chem.* **1999**, *274*, 27815. (d) Wlodawer, A.; Li, M.; Gustchina, A.; Dauter, Z.; Uchida, K.; Oyama, H.; Goldfarb, N. E.; Dunn, B. M.; Oda, K. *Biochemistry* **2001**, *40*, 15602. (e) Wlodawer, A.; Li, M.; Gustchina, A.; Oyama, H.; Oda, K.; Beyer, B. B.; Clemente, J.; Dunn, B. M. *Biochem. Biophys. Res. Commun.* **2004**, *314*, 638.

(6) Bravaya, K.; Bochenkova, A.; Grigorenko, B.; Topol, I.; Burt, S.; Nemukhin, A. *J. Chem. Theory Comput.* **2006**, *2*, 1168.

(7) (a) Wlodawer, A.; Li, M.; Gustchina, A.; Tsuruoka, N.; Ashida, M.; Minakata, H.; Oyama, H.; Oda, K.; Nishino, T.; Nakayama, T. *J. Biol. Chem.* **2004**, *279*, 21500. (b) Comellas-Bigler, M.; Fuentes-Prior, P.; Maskos, K.; Huber, R.; Oyama, H.; Uchida, K.; Dunn, B. M.; Oda, K.; Bode, W. *Structure* **2002**, *10*, 865. (c) Comellas-Bigler, M.; Maskos, K.; Huber, R.; Oyama, H.; Oda, K.; Bode, W. *Structure* **2004**, *12*, 1313. (d) Guhaniyogi, J.; Sohar, I.; Das, K.; Stock, A. M.; Lobel, P. *J. Biol. Chem.* **2009**, *284*, 3985. (e) Pal, A.; Kraetzner, R.; Gruene, T.; Grapp, M.; Schreiber, K.; Gronborg, M.; Urlaub, H.; Becker, S.; Asif, A. R.; Gartner, J.; Sheldrick, G. M.; Steinfeld, R. *J. Biol. Chem.* **2009**, *284*, 3976.

(8) (a) Guo, H.-B.; Wlodawer, A.; Guo, H. *J. Am. Chem. Soc.* **2005**, *127*, 15662. (b) Guo, H.-B.; Wlodawer, A.; Nakayama, T.; Xu, Q.; Guo, H. *Biochemistry* **2006**, *45*, 9129. (c) Xu, Q.; Guo, H.; Wlodawer, A. *J. Am. Chem. Soc.* **2006**, *128*, 5994. (d) Xu, Q.; Guo, H. B.; Wlodawer, A.; Nakayama, T.; Guo, H. *Biochemistry* **2007**, *46*, 3784. (e) Xu, Q.; Li, L. Y.; Guo, H. *J. Phys. Chem. B* **2010**, *114*, 10594.

(9) MOE 2008.

(10) (a) Jorgensen, W. L.; Chandrasekhar, J.; Madura, J. D.; Impey, R. W.; Klein, M. L. *J. Chem. Phys.* **1983**, *79*, 926. (b) Neria, E.; Fischer, S.; Karplus, M. *J. Chem. Phys.* **1996**, *105*, 1902.

(11) Brooks, B. R.; Bruccoleri, R. E.; Olafson, B. D.; States, D. J.; Swaminathan, S.; Karplus, M. *J. Comput. Chem.* **1983**, *4*, 187.

(12) Brooks, C. L.; Brunger, A.; Karplus, M. *Biopolymers* **1985**, *24*, 843.

(13) Cui, Q.; Elstner, M.; Kaxiras, E.; Frauenheim, T.; Karplus, M. *J. Phys. Chem. B* **2001**, *105*, 569.

(14) (a) Elstner, M.; Cui, Q.; Munih, P.; Kaxiras, E.; Frauenheim, T.; Karplus, M. *J. Comput. Chem.* **2003**, *24*, 565. (b) Konig, P. H.; Hoffmann, M.; Frauenheim, T.; Cui, Q. *J. Phys. Chem. B* **2005**, *109*, 9082. (c) Riccardi, D.; Schaefer, P.; Yang, Y.; Yu, H. B.; Ghosh, N.; Prat-Resina, X.; Konig, P.; Li, G. H.; Xu, D. G.; Guo, H.; Elstner, M.; Cui, Q. *J. Phys. Chem. B* **2006**, *110*, 6458.

(15) MacKerell, A. D.; Bashford, D.; Bellott, M.; Dunbrack, R. L.; Evanseck, J. D.; Field, M. J.; Fischer, S.; Gao, J.; Guo, H.; Ha, S.; Joseph-McCarthy, D.; Kuchnir, L.; Kuczera, K.; Lau, F. T. K.; Mattos, C.; Michnick, S.; Ngo, T.; Nguyen, D. T.; Prodhom, B.; Reiher, W. E.; Roux, B.; Schlenkrich, M.; Smith, J. C.; Stote, R.; Straub, J.; Watanabe, M.; Wiorkiewicz-Kuczera, J.; Yin, D.; Karplus, M. *J. Phys. Chem. B* **1998**, *102*, 3586.

(16) Field, M. J.; Bash, P. A.; Karplus, M. *J. Comput. Chem.* **1990**, *11*, 700.

(17) Torrie, G. M.; Valleau, J. P. *Chem. Phys. Lett.* **1974**, *28*, 578.

(18) Kumar, S.; Bouzida, D.; Swendsen, R. H.; Kollman, P. A.; Rosenberg, J. M. *J. Comput. Chem.* **1992**, *13*, 1011.

(19) Ryckaert, J. P.; Ciccotti, G.; Berendsen, H. J. C. *J. Comput. Phys.* **1977**, *23*, 327.

2476

dx.doi.org/10.1021/jp1122294 |*J. Phys. Chem. B* 2011, 115, 2470–2476